

Variational Quantum Eigensolver Ansatz for the J_1 - J_2 -model

Verena Feulner* and Michael J. Hartmann†

Physics Department, Friedrich-Alexander-Universität Erlangen Nürnberg, Germany

(Dated: May 24, 2022)

The ground state properties of the two-dimensional $J_1 - J_2$ -model are very challenging to analyze via classical numerical methods due to the high level of frustration. This makes the model a promising candidate where quantum computers could be helpful and possibly explore regimes that classical computers cannot reach. The $J_1 - J_2$ -model is a quantum spin model composed of Heisenberg interactions along the rectangular lattice edges and along diagonal edges between next-nearest neighbor spins. We propose an ansatz for the Variational Quantum Eigensolver (VQE) to approximate the ground state of an antiferromagnetic $J_1 - J_2$ -Hamiltonian for different lattice sizes and different ratios of J_1 and J_2 . Moreover, we demonstrate that this ansatz can work without the need for gates along the diagonal next-nearest neighbor interactions. This simplification is of great importance for solid state based hardware with qubits on a rectangular grid, where it eliminates the need for SWAP gates. In addition, we provide an extrapolation for the number of gates and parameters needed for larger lattice sizes, showing that these are expected to grow less than quadratically in the qubit number up to lattice sizes which eventually can no longer be treated with classical computers.

I. INTRODUCTION

The development of quantum hardware has made significant progress in recent years and gate sequences that are impossible or at least extremely challenging to be simulated classically [1, 2] have been realized. These gate sequences were designed for benchmark experiments and do not directly lead to “real world” applications of interest. Yet these achievements started the era of “Noisy Intermediate Scale Quantum Computers (NISQ)” which gives rise to the key question of whether useful applications of quantum computers can be possible without quantum error correction [3].

A class of algorithms, that have been identified as suited for NISQ conditions, are variational quantum algorithms [4–6]. These consist of a parametrized gate sequence, for which the gate-parameters are optimized such that the energy expectation value for a considered Hamiltonian is minimized for the prepared quantum state. Two aspects make these algorithms suited for NISQ conditions. One is the fact, that rather short gate sequences can generate highly complex quantum states [1, 2]. The other is that the optimization uses an energy expectation value as the cost function and thus involves an average over a lot of measurements, leading to some robustness against errors.

Variational quantum algorithms have been considered for applications in quantum chemistry [7], where the fermionic degrees of freedom need to be mapped onto qubits via suitable transformations ensuring the anticommutation relations of fermions. Spin lattice systems in turn allow for a more direct representation on quantum computing hardware. Here, variational quantum eigensolver (VQE) algorithms have for example been consid-

ered for spin models on Kagome and square-octagon lattices [8–11] as well as one-dimensional chains [12].

A model that is particularly suited for being represented on a rectangular grid of qubits, but that at the same time poses significant challenges to classical numerics, is the $J_1 - J_2$ -model [13–17]. Indeed, several developers of superconducting qubit architectures develop rectangular grids that are forward compatible with the surface code architecture for quantum error correction. These are particularly suited for computations for spin lattice models on this type of lattices. The $J_1 - J_2$ -model is a spin model on a rectangular lattice that however features additional anti-ferromagnetic interactions across the diagonals of each plaquette, see figure 1. It can for example be used to describe CuO_2 planes in high- T_c cuprate superconductors [18] or layered materials as $\text{Li}_2\text{VO}(\text{Si,GE})\text{O}_4$ [19] or VOMoO_4 [20]. The model however poses significant challenges to classical numerical approaches and for a specific strength of frustration, $0.4 \gtrsim J_2/J_1 \lesssim 0.6$, its ground state remains subject of intense debate [21].

In this work we develop ansätze for variational algorithms for the two-dimensional $J_1 - J_2$ -model, where we particularly focus on the classically hard parameter regime of $0.4 \gtrsim J_2/J_1 \lesssim 0.6$. Importantly, we find that the diagonal interactions can well be captured without executing two qubit gates directly among the next-nearest neighbor qubits involved in these interactions. Two qubit gates along the edges of the rectangular grid, that can be implemented in a hardware efficient ansatz on architectures with nearest neighbor connectivity, suffice for good accuracy of the ground state approximation. Our ansatz is thus less demanding in terms of required qubit-qubit interactions than for example adiabatic algorithms for preparing desired ground states, which always require an implementation of all qubit-qubit interactions that are present in the considered model. The omission of the next nearest neighbor gates along the diagonals of the lattice leads to a significant reduction of the gate

* verena.vf.feulner@fau.de

† michael.j.hartmann@fau.de

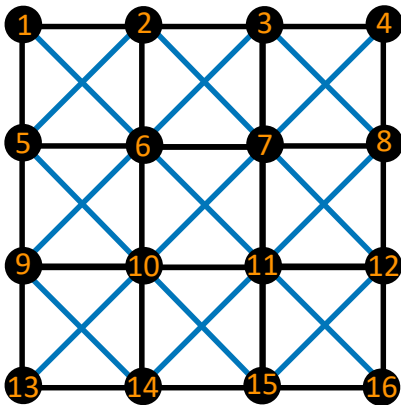


FIG. 1. Interaction geometry for the $J_1 - J_2$ -model on a 16 qubit lattice with open boundary conditions. The blue lines visualize the next-nearest neighbor interactions with a coupling J_2 and the black lines the nearest neighbor interactions with a coupling J_1 .

count, as these gates need to be sandwiched between two SWAP gates in standard architectures with nearest neighbor connectivity.

Furthermore, we explore the scaling of the required numbers of quantum gates for reaching a desired accuracy in the ground state preparation with the number of spins or qubits in the model. For our ansatz without the gates for the next nearest neighbor interactions, we estimate here the promising scaling of $n^{1.2}$, where n is the number of qubits. This scaling implies that $8 \times 8 = 64$ qubit lattices could be treated with circuits containing less than 400 two-qubit gates and less than 100 single qubit gates (We exclude single qubit Z-gates in this counting since these can be done virtually).

II. THE $J_1 - J_2$ -MODEL

The $J_1 - J_2$ -model is an extension of the Heisenberg model with additional Heisenberg-interactions between next-nearest neighbors [22, 23]. The model is described by the Hamiltonian

$$\mathcal{H} = -J_1 \sum_{\langle i,j \rangle} \vec{S}_i \cdot \vec{S}_j - J_2 \sum_{\langle\langle i,j \rangle\rangle} \vec{S}_i \cdot \vec{S}_j, \quad (1)$$

where J_1 is the strength of nearest-neighbor interactions ($\langle i,j \rangle$ indicates that the sum runs over pairs of nearest neighbors) and J_2 is the strength of next-nearest-neighbor interactions ($\langle\langle i,j \rangle\rangle$ indicates that the sum runs over pairs of next-nearest neighbors). The operators \vec{S}_j are vectors containing the three Pauli operators for spin-1/2 degrees of freedom, $\vec{S}_j = (X_j, Y_j, Z_j)^T$. Figure 1 shows the geometry of the spin lattice for 16 spins with open boundary conditions.

In this work the couplings J_1 and J_2 are chosen to be negative and thus, form antiferromagnetic interactions.

The $J_1 - J_2$ -model is a paradigm example for a highly frustrated system, even for the square lattice. Its geometric frustration means that its ground states are typically not formed by simple patterns [24] like, for example, the Néel state, but rather form strongly correlated quantum states. The frustration can be tuned by the ratio J_2/J_1 . For the case of $J_2/J_1 < 0.2$, the model can be described with a spin-wave approximation. For $J_2/J_1 > 0.4$ however, this approximation breaks down [25] and the magnetic order of the model disappears. The following quantum phases of the system have so far been clearly identified: For $J_2/J_1 \lesssim 0.4$, the classical (π, π) Néel behavior is observed. For $J_2/J_1 \gtrsim 0.6$, two collinear Néel ordered states with pitch vectors $q = (\pi, 0)$ and $q = (0, \pi)$ are selected by an order by disorder mechanism. Here, order by disorder means that a soft Ising order parameter $\sigma = \hat{n}_1 \cdot \hat{n}_2$ appears, where \hat{n}_1 and \hat{n}_2 denote the independent staggered magnetization of the two sublattices as written in [26]. The ground state energy is here independent of the angle between the staggered magnetizations [27].

In the highly frustrated case $0.4 \gtrsim J_2/J_1 \lesssim 0.6$, quantum fluctuations destabilize the classical ordered ground state and lead to a disordered singlet ground state with a gap to the first magnetic excitation. Despite significant effort in exploring classical methods the ground state of the model at the maximally frustrated point $J_2/J_1 \sim 0.5$ and its physical properties remain the subject of intense debate [21, 28–31]. So far there have been a few conflicting proposals for the ground state candidate, for instance the plaquette valence-bond state [32], the columnar valence-bond state [33] or a gapless spin liquid [34, 35]. Here the ability of quantum computers to generate highly entangled states already via short gate sequences may lead to an advantage provided the experimental gate fidelities reach suitable values.

III. VARIATIONAL QUANTUM ALGORITHM

Variational quantum algorithms [5, 6] are based on the variational principle in quantum mechanics, which is used to approximate the ground state of a system. This principle reads,

$$E_0 \leq \frac{\langle \psi | \mathcal{H} | \psi \rangle}{\langle \psi | \psi \rangle}, \quad (2)$$

and means that the smallest energy eigenvalue of the system E_0 is always smaller than or equal to any expectation value of its Hamiltonian. This relation gives rise to an optimization problem, in which one seeks to minimize the expectation value of \mathcal{H} for a class of states to find a good approximation to the ground state of \mathcal{H} .

This principle is applied in the Variational Quantum Eigensolver (VQE) [5, 6] to approximate the ground state energy of a given Hamiltonian. The resulting algorithm is a hybrid algorithm that consists of two parts: a classical parameter update and a quantum energy eigenvalue

evaluation. In the quantum part of the algorithm, the expectation value of the Hamiltonian is computed by sampling from an ansatz state $|\psi(\vec{\theta})\rangle$, which is prepared on the quantum processor via a gate sequence that depends on gate parameters $\vec{\theta}$ [5, 6]. The classical parameter update of the algorithm consists of a classical optimizer, which computes the best set of parameters $\vec{\theta}$ by calling the quantum part, to approximate the sought ground state. Thus, the quantum part evaluates the expectation value which forms the objective function for the classical optimizer. By optimizing for better and better sets of parameters, one eventually trains the quantum computer to prepare states that are very close to the ground state of the Hamiltonian.

A. Choosing the ansatz

The ansatz we used for the $J_1 - J_2$ -model is sketched in figure 2. It consists of a parametrized X-gate and a parametrized Y-gate applied to every qubit at the beginning of the circuit. Afterwards, a parametrized Z-gate is applied to each qubit. All these single-qubit gates are parametrized by an angle θ of the rotation around the respective axis. This angle can vary from qubit to qubit. For one qubit the gates read [36],

$$X(\theta) := X^\theta = \begin{pmatrix} G \cdot C & -iG \cdot S \\ -iG \cdot S & G \cdot C \end{pmatrix} \quad (3)$$

$$Y(\theta) := Y^\theta = \begin{pmatrix} G \cdot C & -G \cdot S \\ G \cdot S & G \cdot C \end{pmatrix} \quad (4)$$

$$Z(\theta) := Z^\theta = \begin{pmatrix} 1 & 0 \\ 0 & \tilde{G} \end{pmatrix} \quad (5)$$

where $C = \cos(\pi \cdot \theta/2)$, $S = \sin(\pi \cdot \theta/2)$, $G = \exp(i\pi \cdot \theta/2)$ and $\tilde{G} = \exp(i\pi \cdot \theta)$.

The two-qubit gate, forming the entangling gate in the ansatz, is an “XXYYZZ-gate”, which is applied to every edge of interactions. This “gate” consists of an XX-gate, a YY-gate and a ZZ-gate, all taken to the same power θ , see figure 3. These gates commute and their matrix representations read [37],

$$\text{XX}(\theta) = (X \otimes X)^\theta = \begin{pmatrix} c & 0 & 0 & s \\ 0 & c & s & 0 \\ 0 & s & c & 0 \\ s & 0 & 0 & c \end{pmatrix} \quad (6)$$

$$\text{YY}(\theta) = (Y \otimes Y)^\theta = \begin{pmatrix} c & 0 & 0 & -s \\ 0 & c & s & 0 \\ 0 & s & c & 0 \\ -s & 0 & 0 & c \end{pmatrix} \quad (7)$$

$$\text{ZZ}(\theta) = (Z \otimes Z)^\theta = \begin{pmatrix} 1 & 0 & 0 & 0 \\ 0 & w & 0 & 0 \\ 0 & 0 & w & 0 \\ 0 & 0 & 0 & 1 \end{pmatrix}, \quad (8)$$

with $c = f \cos(\frac{\pi \cdot \theta}{2})$, $s = -if \sin(\frac{\pi \cdot \theta}{2})$, $f = e^{\frac{i\pi \cdot \theta}{2}}$ and $w = e^{i\pi \cdot \theta}$.

The block formed by a layer of Z-gates and a layer of XXYYZZ-gates is then repeated until the desired convergence of the optimizer is reached.

The proposed ansatz consists of the two-qubit gates that correspond to the spin-spin interactions in the Hamiltonian [12, 38, 39] (except for the fact that the gates on the diagonals can be left away). Using these gates has the benefit that they mutually commute. The X- and Y- single qubit gates at the beginning are chosen to mimic the unordered spin-liquid behavior. In Spin-liquids the spins are unordered due to competing interactions hence, their ground state has a high degeneracy. The spins fluctuate heavily, at low temperatures the system can “freeze” to spin glass state [40, 41]. The Hamiltonian is invariant under exchange of the X, Y, and Z directions. In between the two qubit gates we however only use Z-gates since these can be implemented as virtual Z-gates [42] without cost.

Importantly, we found in our simulations that it is possible to omit the gates for the diagonal interactions with strengths J_2 , see green lines in figure 1. This is very useful for the implementation on superconducting quantum hardware due to the fact that superconducting qubits are only coupled to their nearest-neighbours and some superconducting circuit architectures are ordered in a rectangular grid. Thus, if one would aim for simulating the diagonal J_2 interactions directly via gates, SWAP-gates are needed before and after the XXYYZZ-gates. Our ansatz in turn shows that these SWAP gates can be omitted, leading to shorter circuit depth. Our approach thus also has lower hardware connectivity requirements than adiabatic ground state preparation, where all interactions in the model need to be implemented [43].

B. Classical Optimizer

For the classical optimization, the optimizer *Constrained Optimization By Linear Approximation* (COBYLA) was used with randomly chosen initial values for the variational parameters, $-\pi \leq \theta_j \leq \pi$. This optimizing algorithm is a trust-region algorithm that aims to maintain a regular simplex during the iteration steps [44]. This method is nonetheless susceptible to get stuck in local minima in the energy landscape due to the difficulty of the problem. Thus, for a few cases, if necessary, Basinhopping as implemented in SciPy was used. This is a method that uses an arbitrary number of iterations to avoid local minima in the energy landscape, also called basins of attraction. It combines the local optimizer, with a global stepping scheme where all coordinates are displaced by a random number, called step size. The new coordinates are accepted or rejected based on the minimal function value [45].

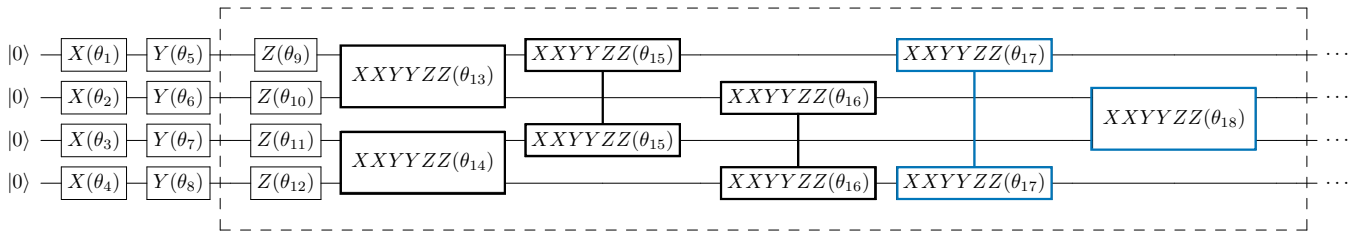


FIG. 2. The ansatz used for the $J_1 - J_2$ -model. Here, the first few gate-layers for a 4-qubit model are shown. The gates in the frame are repeated and we call this block a layer of gates. For the larger models, the ansatz follows the same scheme. The first four two-qubit gates in the block (depicted by bold black frames) are the two-body gates on nearest neighbor qubits. The last two two-qubit gates in the block (depicted by bold blue frames) are the gates on next nearest neighbor qubits along the diagonal interactions. In our simulations, we found that the latter can be omitted without changing the VQE convergence.

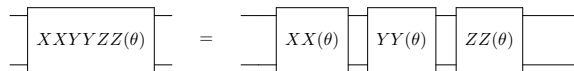


FIG. 3. The parametrized “XXYYZZ”-gate is composed of a sequence of an XX-, YY- and ZZ-gate with the same parameter.

IV. RESULTS

Our main interest is to investigate achievable accuracy as well as the feasibility of our ansatz for a VQE for the simulation of spin glass models. To this end, we have simulated our VQE algorithm for lattices up to 20 spins using a classical computer. As our main interest was the suitability of the ansatz, we computed the energy expectation value of the Hamiltonian directly via the wave function and did not emulate the sampling over measured bit-strings that would be necessary when running the algorithm on a real quantum computer.

Throughout this section, if not stated otherwise, the coupling constants are fixed to the values $J_1 = -1$ and $J_2 = -0.5$. To compare the results, we investigate the achieved energy expectation value \bar{E} and

$$\frac{\bar{E} - E_0}{\text{spectral gap}} = \frac{\bar{E} - E_0}{E_1 - E_0}, \quad (9)$$

that is the difference between the expectation value obtained from the VQE, \bar{E} , and the exact ground state energy E_0 , divided by the spectral gap, which is the difference between the energy of the first excited state E_1 and the ground state energy E_0 .

A. Various lattice sizes

We tested our ansatz with the diagonal gates and without the diagonal gates for different lattice sizes, choosing two-dimensional, rectangular lattices of 12, 16 and 20

qubits with open boundary conditions. The results are shown in figures 4 and 5. Table I shows the number of single and two qubit gates we used in our simulations for the numerical experiments reported in figures 4 and 5. The results \bar{E} that we obtained in these numerical VQE experiments, together with the exact energies of the ground states E_0 , the exact energies of the first excited states E_1 and the ratios $(\bar{E} - E_0)/(E_1 - E_0)$ are reported in table II. Here, we first discuss the simulations that include the gates corresponding to the diagonal J_2 -interactions.

a. Ansatz with diagonal gates For the lattice with 12 qubits with open boundary conditions, we achieve a good convergence within 10^5 iterations. The number of layers (see figure 2) can be seen in table I. The VQE optimization of this lattice can be seen in figure 4. In this case, the ground state can be approximated with $\frac{\bar{E} - E_0}{E_1 - E_0} < 10\%$. For the 16-qubit lattice with open boundary conditions, we found the optimization result as can be seen in table II with seven gates, see table I. Thus, the VQE only ends up in the bottom 20 percent interval of the spectral gap, as can be seen in figure 4. To achieve better results, the ansatz can be extended to more gate layers. In the case of 16-qubits with nearest-neighbor interaction gates we also did not use the basinhopping scheme which might also help to achieve better results.

The largest lattice size we considered was a two-dimensional grid with 20 qubits. Due to the large size of the Hilbert space and the risk of running into local minima of the energy landscape, a good guess for start values of the variational parameters is beneficial. To achieve this, we first ran the VQE with seven gate layers, which resulted in a value for \bar{E} that lies approximately in the middle of the spectral gap. For higher accuracy we fed the obtained set of parameters as an initial guess into our VQE ansatz with 12 ansatz layers, where we set the θ -values for the additional parametrized gates to 10^{-5} [46]. With this approach we get a good approximation of the ground state, albeit at the cost of doubling the number of ansatz-layers.

Overall, we find that due to the parametrized X- and Y-gates at the beginning of the ansatz, the spins in the

	number of 2 qubit gates	number of single qubit gates	number of parameters	number of layer-blocks
12 with diagonal gates	609	108	312	7
12 diag, period. bound.	987	108	431	7
12 without diag. gates	357	108	227	7
16 with diagonal gates	861	144	432	7
16 without diag. gates	288	144	312	7
20 with diagonal gates	1944	280	931	12
first try smaller size	1134	180	558	7
20 without diag. gates	1080	280	640	12
first try smaller size	450	140	290	5

TABLE I. Number of gates, layers and parameters used in the different configurations of the simulation. For the variation of J_2 the same number of gates and layers were used as for the model with 12 qubits with diagonal interactions and without periodic boundaries.

	E_0	E_1	\bar{E}	$\frac{\bar{E}-E_0}{E_1-E_0}$
12 with diagonal gates, $J_2 = 0$	-26.777	-24.879	-26.4375	16 %
12 with diagonal gates, $J_2 = -0.5$	-22.138	-20.1559	-21.980	7.9 %
12 with diagonal gates, $J_2 = -2$	-41.240	-40.479	-40.8734	48 %
12 diag, period. bound.	-25.7220	-23.0742	-25.441	10.6 %
12 without diag. gates	-22.1380	-20.1559	-21.995	7.2 %
16 with diagonal gates	-30.0222	-27.8223	-29.5856	19.9 %
16 without diag. gates	-30.0222	-27.8223	-29.566	20.8 %
20 with diagonal gates	-37.7231	-35.9921	-37.416	17.7 %
20 without diag. gates	-37.7231	-35.9921	-37.459	15.3 %

TABLE II. The results of the various simulations.

$J_1 - J_2$ -model can be prepared in the expected spin liquid order for the ground state or a good approximation of it in most cases of our simulations. In all configurations, we achieve an energy result which is closer to the ground state than the first excited state. The precision of the model could be increased by more gate layers or by the use of a better suited optimizer that is less susceptible to local energy minima and the initial state.

b. Ansatz without diagonal-interaction gates To show that our ansatz works without using gates that mimic the diagonal J_2 -interaction, we implemented the VQE without gates on the diagonals for lattices of 12, 16 and 20 qubits with open boundary conditions. The results of these simulations can also be found in table II. The ansatz here follows the same scheme as above, except for not applying diagonal interactions via gates on next-nearest neighbor qubits (blue boxes in figure 2). Leaving out these gates reduces the gate count in two ways. Firstly the omitted gates need not be implemented and secondly these gates would need to be sandwiched between SWAP gates in architectures with only nearest neighbor connectivity as they cannot be implemented directly.

For this ansatz, we get a slightly better results in the optimization for all considered lattice sizes, as can be seen in figure 5 and table II. This could be due to the fact that fewer parameters are used and the optimizer is more efficient in finding a minimum. The only case, where the value is slightly worse than for the ansatz with diagonal gates, is the 16-qubit lattice, which might be due to the fact that a better initial state for the optimization was

found in the run that included gates on the diagonals. In the cases of 12 and 16 qubits we also needed fewer iterations. In turn, the slightly increased number of iterations needed for the 20 qubit optimization is caused by the fact that only five layers of gates were here used in the "pre-training" stage (as compared to seven layers in the case with gates on the diagonals). Hence, the training of the full 12 layer circuit in the second training stage required more iterations.

c. Further ground state properties With the wave function output of our full wave function VQE simulation, we can also calculate expectation values of other physical observables to confirm that the prepared state captures well the properties of the exact ground state. As an example, we calculated the spin-spin correlation in x -direction $\langle \sigma_i^x \sigma_j^x \rangle$ for the 12-qubit lattice without diagonal gates and for open boundary conditions. We compare the result with the spin-spin correlation function of the exact result and calculate the difference, as can be seen in figure 6. We can see a very good agreement, showing that the VQE approximation is indeed very accurate.

B. Variation of J_2

To explore how good the ansatz performs for different values of the ratio of the couplings J_2/J_1 , and therefore for different quantum phases of the model, we here show results for a fixed value of $J_1 = -1$ where we varied the value of J_2 , see figure 7. We choose the range of J_2 values such that the different quantum phases of the $J_1 - J_2$ -

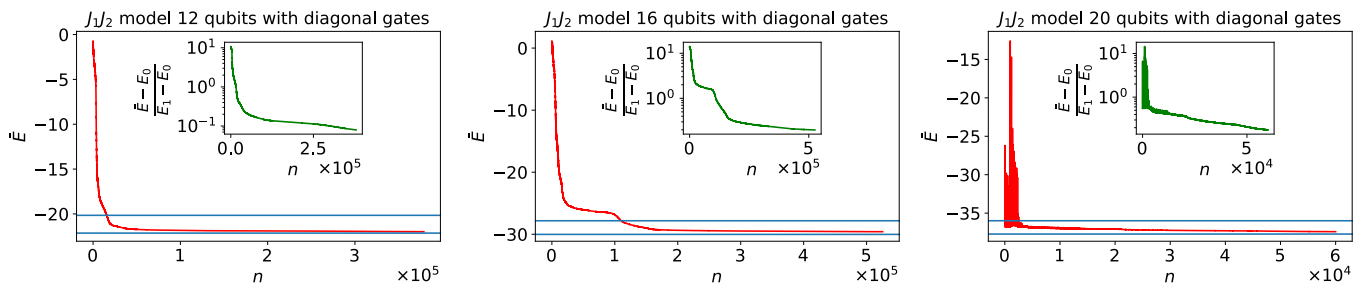


FIG. 4. VQE performance for the $J_1 - J_2$ -model for all lattice sizes (12,16 and 20) without periodic boundary conditions and with diagonal gates. The lower blue line marks the ground state energy E_0 and the upper line the energy of the first excited state E_1 . The circuit consists of the additional X- and Y-layer at the beginning plus the according number of layers, as can be seen in table I. The inset shows the run of the VQE-steps against the difference of the expectation value \bar{E} from the VQE and the exact ground state energy E_0 divided by the spectral gap, which is the difference of the energy of the first excited state E_1 and the ground state energy.

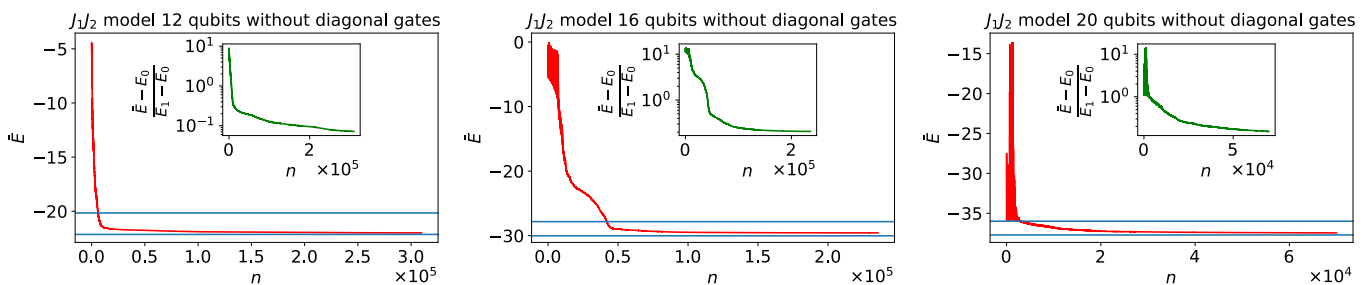


FIG. 5. VQE performance for the $J_1 - J_2$ -model for all lattice sizes (12,16 and 20) without periodic boundary conditions and without diagonal gates. The lower blue line marks the ground state energy E_0 and the upper line the energy of the first excited state E_1 . The circuit consists of the additional X- and Y-layer at the beginning plus the according number of layers, as can be seen in table I. The inset shows the run of the VQE-steps against the difference of the expectation value \bar{E} from the VQE and the exact ground state energy E_0 divided by the spectral gap, which is the difference of the energy of the first excited state E_1 and the ground state energy.

model are covered. For the collinear Néel ordered states we choose $J_2 = -2$ and for the Néel ordered ground state $J_2 = 0$, which thus corresponds to the Heisenberg model. The obtained values for the energies \bar{E} can be found in table II.

For all choices of J_2 , our ansatz achieves a good convergence to the respective ground state. For the ground state energy for the VQE with $J_2 = 0$, we achieve a value of 16% of the spectral gap. For $J_2 = -2$ the VQE achieved a value of only 48% of the spectral gap. We note that a good convergence in terms of the spectral gap is in this case difficult to achieve because the spectral gap is very small. Nonetheless, the achieved energy is close to the ground state energy. Our findings are thus in agreement with the generic behavior that in cases where the spectral gap is narrow, more gate layers have to be used to achieve a higher accuracy. We can thus see that the ansatz is rather versatile and yields good approximations for all phases of the model. We attribute this good performance to the choice of the ansatz, including the parametrized X- and Y-gates at the beginning of the circuit.

C. Extrapolation of parameter-numbers for larger lattice sizes

The effort of running a VQE algorithm is determined by the number of gates that are needed, since this number determines the hardware requirements, and the number of variational parameters that are needed, since this number determines the number of optimization steps and thus the number of required measurements.

To estimate how many gates and how many variational parameters are needed in our ansatz for larger systems, we plotted the number of required gate numbers and variational parameters for the system sizes for which we did our simulations and extrapolated the resulting curve for each ansatz. As a criterion for successful convergence, we require that the achieved expectation value \bar{E} is lower or equal to the middle of the spectral gap $E_1 - E_0$. We then determine the minimal number of gate layers or minimal number of gates needed to achieve this, and plot the corresponding number of two-qubit gates and variational parameters numbers for all lattice sizes for which we can simulate the algorithm classically. By fitting a polynomial to this data, we extrapolate the expected required

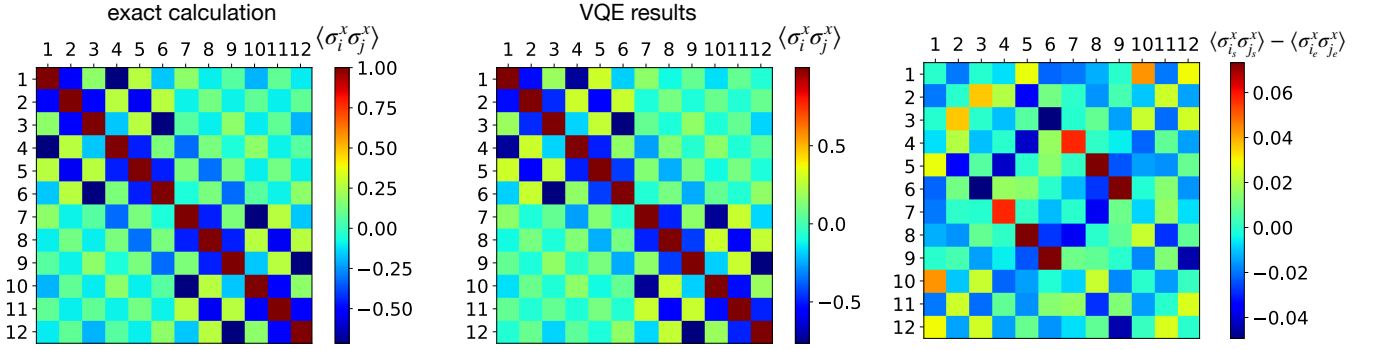


FIG. 6. Spin-spin correlation in x -direction $\langle \sigma_i^x \sigma_j^x \rangle$ for the 12-qubit lattice without diagonal gates computed from the final state of the corresponding simulation reported in table II and figure 5. The plot on the left shows the correlation function calculated with the VQE-results. The middle plot is the correlation function of the exact results, and on the right the difference of both can be seen. Subscript s are the results of the VQE simulation and e are the exact results.

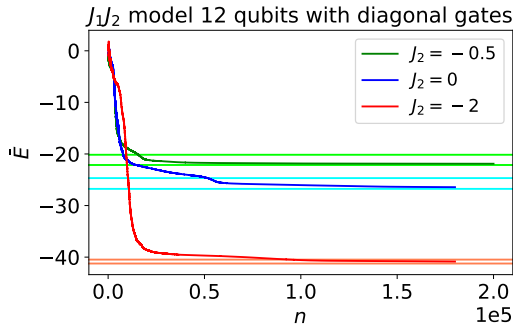


FIG. 7. VQE performance for the $J_1 - J_2$ -model with 12 qubits without diagonal interaction gates. The lighter lines mark the ground state energy E_0 and energy of the first excited state E_1 . The circuit for each configuration of J_2 consists of 7 gate layers plus the additional X- and Y-layer at the beginning.

number of two-qubit gates and variational parameters to larger lattice sizes.

The number of required gates to achieve $\bar{E} \leq 0.5 \cdot E_1 - E_0$ for the efficient ansatz without diagonal gates is shown in figure 8. We find a $n^{1.2}$ dependency on the qubit number. These gate numbers correspond to the required number of gate layers as shown in figure 9, which is identical of both ansätze (with and without diagonal gates) due to the definition of gate layer that we use. Interestingly, the number of required layers grows less than linear in the number of qubits, which is a promising behavior for scalability.

The number of required variational parameters to achieve $\bar{E} \leq 0.5 \cdot E_1 - E_0$ is shown in figure 10 for the ansatz with next-nearest neighbor gates and in figure 11 for the ansatz without next-nearest neighbor gates. With our extrapolation procedure, we find a $n^{1.5}$ dependency on the qubit number n for the number of parameters of the ansatz with diagonal interaction gates and a dependency of $n^{1.2}$ for the ansatz without the diagonal inter-

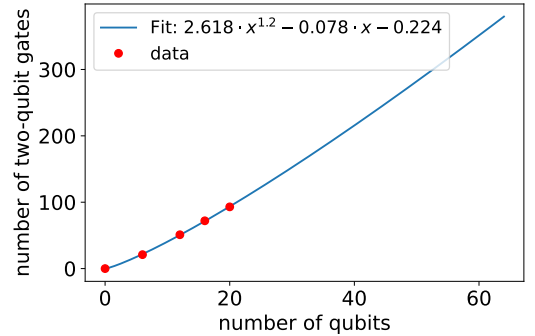


FIG. 8. Number of two-qubit gates required in our numerical studies using the ansatz without diagonal-interaction gates to achieve $\bar{E} \leq 0.5 \cdot E_1 - E_0$ (red dots) for different lattice sizes and fit to this data (blue line). The extrapolation of the fit shows the expected number of two-qubit gates for up to 64 qubits (corresponding to an 8×8 qubit grid). We find a $x^{1.2}$ -growth of the required number of parameters. The number of two-qubit gates here is the sum of all XX-, YY- and ZZ-gates used to achieve the required convergence.

action gates. Hence, the curve for the ansatz without the diagonal gates increases more slowly than for the ansatz with diagonal gates. This observation indicates that omitting the diagonal gates can lead to a significant reduction in the depth of the ansatz and thus the circuit, as one increases the size of the spin lattice.

V. CONCLUSIONS

We simulated and tested a Variational Quantum Eigensolver for the two-dimensional $J_1 - J_2$ -model. Using the proposed ansatz, one can access the ground state energy of this spin-model. Moreover, our ansatz can be used without gates that directly implement the diagonal next-nearest neighbor interactions. This feature allows to avoid SWAP gates when executing the gate se-

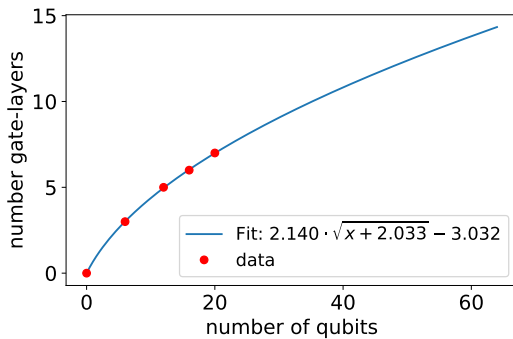


FIG. 9. Number of gate layers required in our numerical studies to achieve $\bar{E} \leq 0.5 \cdot E_1 - E_0$ (red dots) for different lattice sizes and fit to this data (blue line). The extrapolation of the fit shows the expected number of gate layers for up to 64 qubits (corresponding to an 8×8 qubit grid). We find a \sqrt{x} -growth of the required number of parameters. This plot is valid for both ansätze (with and without diagonal gates).

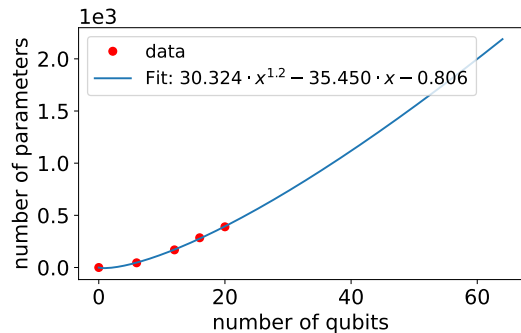


FIG. 11. Number of variational parameters used in our numerical studies using the ansatz without diagonal-interaction gates for different lattice sizes (red dots) and fit to this data (blue line). The extrapolation of the fit shows the expected number of parameters for up to 64 qubits (corresponding to an 8×8 qubit grid). Using this extrapolation, we find an $x^{1.2}$ -growth of the required number of parameters.

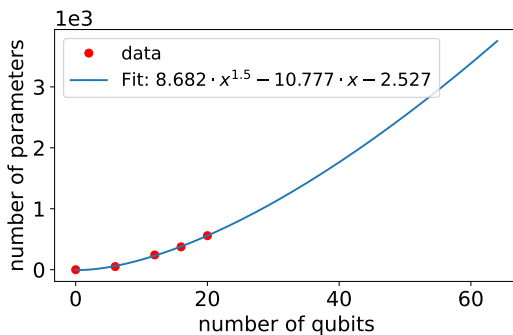


FIG. 10. Number of variational parameters used in our numerical studies using the ansatz with diagonal-interaction gates for different lattice sizes (red dots) and fit to this data (blue line). The extrapolation of the fit shows the expected number of parameters for up to 64 qubits (corresponding to an 8×8 qubit grid). We find an $x^{1.5}$ -growth of the required number of parameters.

quence on hardware with qubits on a rectangular grid that can only undergo gate operations with their nearest neighbors. Moreover, we analyzed the different quantum phases in the $J_1 - J_2$ -model model by varying J_2/J_1 . We saw that our ansatz worked well for all the different configurations and led to a sufficient accuracy in the ground state approximation. To improve the performance, a better suited optimizer than COBYLA or more basin-hopping iterations could be used to avoid getting stuck in energy plateaus or local minima. Another option to improve the performance, are greater circuit depths with more parameters or a more suitable initial configuration that already displays some information about the system.

By fitting a polynomial to the required number of two-qubit gates and the required number of variational parameters versus qubit number, we anticipate that the re-

quired number of two-qubit gates and parameters grow slower than quadratically in the number of qubits. While the required number of gates can not yet be run with sufficient accuracy on existing hardware, successful VQE implementations that eventually may challenge results of classical numerics thus seem within reach in the near future.

ACKNOWLEDGMENTS

This work received support from the German Federal Ministry of Education and Research via the funding program quantum technologies - from basic research to the market under contract number 13N15684 “GeQCoS” and under contract number 13N15577 “MANIQU”. It is also part of the Munich Quantum Valley, which is supported by the Bavarian state government with funds from the Hightech Agenda Bayern Plus.

Appendix A: Details of the Simulation

The simulation of the Variational Quantum Eigensolver for the $J_1 - J_2$ -model was done in Python 3.8.5 with the help of NumPy 1.20.2 [47] using Cirq 0.10.0 [36]. For the optimization, the built-in optimizers from SciPy 1.6.3 [48] were used. We used the gate `cirq.X(q)`, `cirq.Y(q)`, `cirq.Z(q)`, `cirq.XX(q1,q2)`, `cirq.YY(q1,q2)` and `cirq.ZZ(q1,q2)` built in Cirq to a power of the respective parameter. And defined the Hamiltonian via Pauli operators in Cirq via `cirq.PauliSum`. After applying a sufficient amount of gate-repetitions, the circuit was simulated. We used `qsimcirq`, a full wave function simulator written in C++ which is much faster than the normal simulator in Cirq.

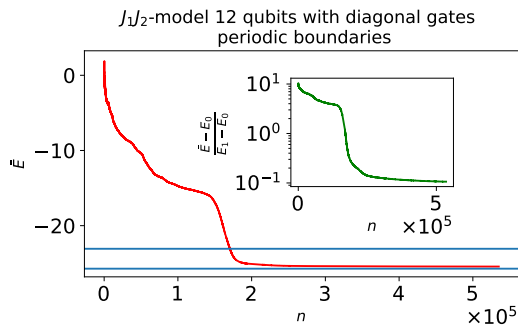


FIG. 12. VQE performance for the $J_1 - J_2$ -model with 12 qubits with periodic boundary conditions. The lower blue line marks the ground state energy E_0 and the upper line the energy of the first excited state E_1 . The circuit consists of 7 layers of gates plus the additional X- and Y-layer at the beginning. The inset shows the run of the VQE-steps against the difference of the expectation value \bar{E} from the VQE and the exact ground state energy E_0 divided by the spectral gap, which is the difference of the energy of the first excited state E_1 and the ground state energy.

Appendix B: Results for periodic boundary conditions

For the 12-qubit model we also tested if the ansatz works for a lattice with periodic boundary conditions (In figure 1 periodic boundaries would mean for example a J_1 interaction between qubits 1 and 4, 1 and 13. As well as J_2 interactions, e.g. of qubits 1 and 14 and qubits 2 and 13).

For this lattice with periodic boundary conditions, the exact values for the ground and first excited state energies can be found in table II. We achieve a value for \bar{E} for which $\frac{\bar{E}-E_0}{E_1-E_0} < 10\%$. We thus conclude that our ansatz also works with periodic boundary conditions and the same number of gate layers (see table I) as for the lattice with open boundaries.

-
- [1] F. Arute, K. Arya, R. Babbush, D. Bacon, J. Bardin, R. Barends, R. Biswas, S. Boixo, F. Brandao, D. Buell, B. Burkett, Y. Chen, J. Chen, B. Chiaro, R. Collins, W. Courtney, A. Dunsworth, E. Farhi, B. Foxen, A. Fowler, C. M. Gidney, M. Giustina, R. Graff, K. Guerin, S. Habegger, M. Harrigan, M. Hartmann, A. Ho, M. R. Hoffmann, T. Huang, T. Humble, S. Isakov, E. Jeffrey, Z. Jiang, D. Kafri, K. Kechedzhi, J. Kelly, P. Klimov, S. Knysh, A. Korotkov, F. Kostritsa, D. Landhuis, M. Lindmark, E. Lucero, D. Lyakh, S. Mandrà, J. R. McClean, M. McEwen, A. Megrant, X. Mi, K. Michielsen, M. Mohseni, J. Mutus, O. Naaman, M. Neeley, C. Neill, M. Y. Niu, E. Ostby, A. Petukhov, J. Platt, C. Quintana, E. G. Rieffel, P. Roushan, N. Rubin, D. Sank, K. J. Satzinger, V. Smelyanskiy, K. J. Sung, M. Trevithick, A. Vainsencher, B. Villalonga, T. White, Z. J. Yao, P. Yeh, A. Zalcman, H. Neven, and J. Martinis, Quantum supremacy using a programmable superconducting processor, *Nature* **574**, 505–510 (2019).
- [2] Y. e. a. Wu, Strong quantum computational advantage using a superconducting quantum processor, *Phys. Rev. Lett.* **127**, 180501 (2021).
- [3] K. Bharti, A. Cervera-Lierta, T. H. Kyaw, T. Haug, S. Alperin-Lea, A. Anand, M. Degroote, H. Heimonen, J. S. Kottmann, T. Menke, W.-K. Mok, S. Sim, L.-C. Kwek, and A. Aspuru-Guzik, Noisy intermediate-scale quantum algorithms, *Rev. Mod. Phys.* **94**, 015004 (2022).
- [4] M. Cerezo, A. Arrasmith, R. Babbush, S. C. Benjamin, S. Endo, K. Fujii, J. R. McClean, K. Mitarai, X. Yuan, L. Cincio, and P. J. Coles, Variational quantum algorithms, *Nature Reviews Physics* **3**, 625 (2021).
- [5] A. Peruzzo, J. McClean, P. Shadbolt, M.-H. Yung, X.-Q. Zhou, P. J. Love, A. Aspuru-Guzik, and J. L. O’Brien, A variational eigenvalue solver on a photonic quantum processor, *Nature Communications* **5** (2014).
- [6] J. McClean, J. Romero, R. Babbush, and A. Aspuru-Guzik, The theory of variational hybrid quantum-classical algorithms, *New Journal of Physics* **18** (2015).
- [7] S. McArdle, S. Endo, A. Aspuru-Guzik, S. C. Benjamin, and X. Yuan, Quantum computational chemistry, *Reviews of Modern Physics* **92**, 10.1103/revmodphys.92.015003 (2020).
- [8] J. Kattemölle and J. van Wezel, Variational quantum eigensolver for the heisenberg antiferromagnet on the kagome lattice (2021).
- [9] J. L. Bosse and A. Montanaro, Probing ground state properties of the kagome antiferromagnetic heisenberg model using the variational quantum eigensolver (2021).
- [10] A. C. Y. Li, M. S. Alam, T. Iadecola, A. Jahin, D. M. Kurkcuoglu, R. Li, P. P. Orth, A. B. Özgüler, G. N. Perdue, and N. M. Tubman, Benchmarking variational quantum eigensolvers for the square-octagon-lattice kitaev model (2021).
- [11] T. A. Bespalova and O. Kyriienko, Quantum simulation and ground state preparation for the honeycomb kitaev model (2021).
- [12] K. Seki, T. Shirakawa, and S. Yunoki, Symmetry-adapted variational quantum eigensolver, *Phys. Rev. A* **101**, 052340 (2020).
- [13] W.-J. Hu, F. Becca, A. Parola, and S. Sorella, Direct evidence for a gapless Z_2 spin liquid by frustrating néel antiferromagnetism, *Phys. Rev. B* **88**, 10.1103/PhysRevB.88.060402 (2013).
- [14] T. Nakamura and N. Hatano, Quantum monte carlo calculation of the j1-j2 model, *Journal of the Physical Society of Japan* **62**, 10.1143/JPSJ.62.3062 (1993).
- [15] A. Kalz, A. Honecker, and M. Moliner, Analysis of the phase transition for the ising model on the frustrated square lattice, *Phys. Rev. B* **84**, 10.1103/PhysRevB.84.174407 (2011).

- [16] D. Hangleiter, I. Roth, D. Nagaj, and J. Eisert, Easing the monte carlo sign problem, *Science Advances* **6**, 10.1126/sciadv.abb8341 (2020).
- [17] J. Hasik, D. Poilblanc, and F. Becca, Investigation of the néel phase of the frustrated heisenberg antiferromagnet by differentiable symmetric tensor networks, *SciPost Physics* **10**, 10.21468/scipostphys.10.1.012 (2021).
- [18] A. Mikheyenkov, A. V. Shvartsberg, and A. Barabanov, Phase transitions in the 2d j_1 - j_2 heisenberg model with arbitrary signs of exchange interactions, *JETP Letters* **98**, 156 (2013).
- [19] N. Papinutto, P. Carretta, S. Gonthier, and P. Millet, Spin dilution in frustrated two-dimensional $s = \frac{1}{2}$ antiferromagnets on a square lattice, *Phys. Rev. B* **71**, 10.1103/PhysRevB.71.174425 (2005).
- [20] P. Carretta, N. Papinutto, C. B. Azzoni, M. C. Mozzi, E. Pavarini, S. Gonthier, and P. Millet, Frustration-driven structural distortion in VMOO_4 , *Phys. Rev. B* **66**, 10.1103/PhysRevB.66.094420 (2002).
- [21] K. Choo, T. Neupert, and G. Carleo, Two-dimensional frustrated J_1 - J_2 model studied with neural network quantum states, *Phys. Rev. B* **100**, 125124 (2019).
- [22] D. Roscher, N. Gneist, M. M. Scherer, S. Trebst, and S. Diehl, Cluster functional renormalization group and absence of a bilinear spin liquid in the J_1 - J_2 heisenberg model, *Phys. Rev. B* **100** (2019).
- [23] M. Mambrini, A. Läuchli, D. Poilblanc, and F. Mila, Plaquette valence-bond crystal in the frustrated heisenberg quantum antiferromagnet on the square lattice, *Phys. Rev. B* **74** (2006).
- [24] J.-F. Sadoc and R. Mosseri, *Geometrical Frustration*, Collection Alea-Saclay: Monographs and Texts in Statistical Physics (Cambridge University Press, 1999).
- [25] Q. F. Zhong and S. Sorella, Spin-wave theory on finite lattices: Application to the j_1 - j_2 heisenberg model, *Europhysics Letters (EPL)* **21**, 629 (1993).
- [26] P. Chandra, P. Coleman, and A. I. Larkin, Ising transition in frustrated heisenberg models, *Phys. Rev. Lett.* **64** (1990).
- [27] E. Dagotto and A. Moreo, Phase diagram of the frustrated spin-1/2 heisenberg antiferromagnet in 2 dimensions, *Phys. Rev. Lett.* **63**, 2148 (1989).
- [28] L. Isaev, G. Ortiz, and J. Dukelsky, Hierarchical mean-field approach to the J_1 - J_2 heisenberg model on a square lattice, *Phys. Rev. B* **79**, 10.1103/PhysRevB.79.024409 (2009).
- [29] M. Hering, J. Sonnenschein, Y. Iqbal, and J. Reuther, Characterization of quantum spin liquids and their spinon band structures via functional renormalization, *Phys. Rev. B* **99**, 100405 (2019).
- [30] Y. Nomura, Helping restricted boltzmann machines with quantum-state representation by restoring symmetry, *Journal of Physics: Condensed Matter* **33**, 174003 (2021).
- [31] Y. Nomura and M. Imada, Dirac-type nodal spin liquid revealed by refined quantum many-body solver using neural-network wave function, correlation ratio, and level spectroscopy, *Physical Review X* **11**, 10.1103/physrevx.11.031034 (2021).
- [32] L. Capriotti and S. Sorella, Spontaneous plaquette dimerization in the $j_1 - j_2$ heisenberg model, *Phys. Rev. Lett.* **84** (2000).
- [33] R. R. P. Singh, Z. Weihong, C. J. Hamer, and J. Oitmaa, Dimer order with striped correlations in the J_1 - j_2 heisenberg model, *Phys. Rev. B* **60** (1999).
- [34] L. Wang, D. Poilblanc, Z.-C. Gu, X.-G. Wen, and F. Verstraete, Constructing a gapless spin-liquid state for the spin-1/2 $J_1 - J_2$ heisenberg model on a square lattice, *Phys. Rev. Lett.* **111** (2013).
- [35] P. W. Anderson, The resonating valence bond state in $\text{La}_{2-x}\text{Cu}_x\text{O}_7$ and superconductivity, *Science* **235**, 10.1126/science.235.4793.1196 (1987).
- [36] C. Developers, *Cirq* (2021), See full list of authors on Github: <https://github.com/quantumlib/Cirq/graphs/contributors>.
- [37] <https://quantumai.google/reference/python/cirq/ops/XXPowGate>, <https://quantumai.google/reference/python/cirq/ops/XX>, <https://quantumai.google/reference/python/cirq/ops/YPowGate>, <https://quantumai.google/reference/python/cirq/ops/YY>, <https://quantumai.google/reference/python/cirq/ops/ZZPowGate>, <https://quantumai.google/reference/python/cirq/ops/ZZ>, accessed: 2022-04-04.
- [38] J.-G. Liu, Y.-H. Zhang, Y. Wan, and L. Wang, Variational quantum eigensolver with fewer qubits, *Physical Review Research* **1**, 10.1103/physrevresearch.1.023025 (2019).
- [39] D. Huerga, Variational quantum simulation of valence-bond solids (2022).
- [40] A. Sen and R. Moessner, Topological spin glass in diluted spin ice, *Phys. Rev. Lett.* **114**, 247207 (2015).
- [41] L. Balents, Spin liquids in frustrated magnets, *Nature* **464**, 199 (2010).
- [42] D. C. McKay, C. J. Wood, S. Sheldon, J. M. Chow, and J. M. Gambetta, Efficient z gates for quantum computing, *Phys. Rev. A* **96**, 022330 (2017).
- [43] T. Albash and D. A. Lidar, Adiabatic quantum computation, *Rev. Mod. Phys.* **90**, 015002 (2018).
- [44] M. J. D. Powell, A direct search optimization method that models the objective and constraint functions by linear interpolation, in *Advances in Optimization and Numerical Analysis* (1994) pp. 51–67.
- [45] D. J. Wales and J. P. K. Doye, Global optimization by basin-hopping and the lowest energy structures of lennard-jones clusters containing up to 110 atoms, *The Journal of Physical Chemistry A* **101** (1997).
- [46] Setting these exactly to zero led to numerics problems, presumably because of hitting a fix-point of the optimizer.
- [47] C. R. Harris, K. J. Millman, S. J. van der Walt, R. Gommers, P. Virtanen, D. Cournapeau, E. Wieser, J. Taylor, S. Berg, N. J. Smith, R. Kern, M. Picus, S. Hoyer, M. H. van Kerkwijk, M. Brett, A. Haldane, J. F. del Río, M. Wiebe, P. Peterson, P. Gérard-Marchant, K. Sheppard, T. Reddy, W. Weckesser, H. Abbasi, C. Gohlke, and T. E. Oliphant, Array programming with NumPy, *Nature* **585** (2020).
- [48] P. Virtanen, R. Gommers, T. E. Oliphant, M. Haberland, T. Reddy, D. Cournapeau, E. Burovski, P. Peterson, W. Weckesser, J. Bright, S. J. van der Walt, M. Brett, J. Wilson, K. J. Millman, N. Mayorov, A. R. J. Nelson, E. Jones, R. Kern, E. Larson, C. J. Carey, Í. Polat, Y. Feng, E. W. Moore, J. VanderPlas, D. Laxalde, J. Perktold, R. Cimrman, I. Henriksen, E. A. Quintero, C. R. Harris, A. M. Archibald, A. H. Ribeiro, F. Pedregosa, P. van Mulbregt, and SciPy 1.0 Contributors, SciPy 1.0: Fundamental Algorithms for Scientific Computing in Python, *Nature Methods* **17** (2020).